



Original Article

Seismic fragility evaluation of the base-isolated nuclear power plant piping system using the failure criterion based on stress-strain

Sung-Wan Kim ^a, Bub-Gyu Jeon ^{a,*}, Dae-Gi Hahm ^b, Min-Kyu Kim ^b^a Seismic Research and Test Center, Pusan National University, 49 Busandaehak-ro, Mugeum, Yangsan, Kyungnam, 50612, Republic of Korea^b Integrated Safety Assessment Division, Korea Atomic Energy Research Institute, 111 Daedeok-daero 989 beon-gil, Yusung-gu, Daejon, 34057, Republic of Korea

article info

Article history:

Received 29 August 2018

Received in revised form

4 October 2018

Accepted 8 October 2018

Available online 9 October 2018

Keywords:

Nuclear power plant piping system

Steel pipe elbow

Damage index

Seismic fragility analysis

BNL-NRC benchmark model

abstract

In the design criterion for the nuclear power plant piping system, the limit state of the piping against an earthquake is assumed to be plastic collapse. The failure of a common piping system, however, means the leakage caused by the cracks. Therefore, for the seismic fragility analysis of a nuclear power plant, a method capable of quantitatively expressing the failure of an actual piping system is required. In this study, it was conducted to propose a quantitative failure criterion for piping system, which is required for the seismic fragility analysis of nuclear power plants against critical accidents. The in-plane cyclic loading test was conducted to propose a quantitative failure criterion for steel pipe elbows in the nuclear power plant piping system. Nonlinear analysis was conducted using a finite element model, and the results were compared with the test results to verify the effectiveness of the finite element model. The collapse load point derived from the experiment and analysis results and the damage index based on the stress-strain relationship were defined as failure criteria, and seismic fragility analysis was conducted for the piping system of the BNL (Brookhaven National Laboratory) - NRC (Nuclear Regulatory Commission) benchmark model.

© 2018 Korean Nuclear Society. Published by Elsevier Korea LLC. This is an open access article under the CC BY-NC-ND license (<http://creativecommons.org/licenses/by-nc-nd/4.0/>).

1. Introduction

The interest in the seismic safety of nuclear power plant facilities has been growing of late, ever since the Great East Japan earthquake occurred. As nuclear power plants are subject to larger damage intensity and extent than any other infrastructure when natural disasters like earthquakes occur, their safety is emphasized more than anything else [1]. As it is practically impossible to accurately predict the occurrence timing and intensity of a natural disaster [2,3], it is necessary to set the scope of potential natural disasters and to minimize the damage by improving the resistance capabilities of the structures based on the scope. Thus, when nuclear power plants are built in areas where strong earthquakes frequently occur, seismic design as well as the application of seismic isolation devices is essential [4].

Seismic isolation devices ensure safety by absorbing the ground motion when an earthquake affects the structures, and have been applied to various infrastructures. They are installed in the

boundary between the lower part of a structure and the upper part of the ground, and decrease the effect of the seismic load by increasing the natural frequency of the upper structure in the event of an earthquake [5,6]. Studies on the application of seismic isolation devices have been conducted of late to secure safety against earthquakes. In France, seismic isolation devices have already been introduced to nuclear power plants since the 1980s, and such nuclear power plants are still in commercial operation. In Japan and the U.S., research is actively being conducted to prepare independent guidelines on the installation of seismic isolation devices in nuclear power plants.

In South Korea, seismic isolation devices have been applied to the bottom of the reactor containment building (RCB) and auxiliary building (AB) of APR1400 - Korean Standard Nuclear Power Plant (Advanced Power Reactor 1400), a new nuclear power plant model, since 2011. In the design of a base-isolated nuclear power plant, the seismic design of an interface piping system that supports both a structure with seismic isolation devices and a structure without seismic isolation devices is important. In the event of an earthquake, the interface piping system is deformed by a large relative displacement between the structure with seismic isolation devices

* Corresponding author.

E-mail address: bkjeon79@pusan.ac.kr (B.-G. Jeon).

and the structure without seismic isolation devices. At the same time, it is excited by the two buildings with different vibration characteristics. For the seismic design of the interface piping system, a stiffness level capable of accepting inertial forces caused by the different excitation characteristics of the buildings due to the installation of seismic isolation devices is required. In addition, it is necessary to consider flexibility, which can allow a large relative displacement between these buildings caused by an earthquake. The seismic risk may increase due to the repeated application of external forces determined by the natural period of the seismic isolation device and the seismic anchor motion of the connected section. For example, as the main steam piping of the APR 1400 nuclear power plant connects an RCB with seismic isolation devices and a turbine building (TB) without seismic isolation devices, the interface piping is likely to be damaged by the application of external forces with low frequencies at the connection section. Therefore, research is required for the selection of facilities whose seismic risks are increased by the installation of seismic isolation devices, and for verifying the performance of each facility by calculating their seismic risks. As seismic isolation systems are applied to nuclear power plants, studies have been conducted to develop numerical procedures for the computation of the seismic fragilities of equipment and structural components for isolated buildings [7,8]. Studies have also been conducted to improve the seismic performances of nuclear power plants while minimizing the design changes for the application of seismic isolation devices [9]. A seismic fragility analysis method for nuclear power plants with seismic isolation devices was developed, and the seismic safety of the APR1400 nuclear power plant was evaluated by conducting seismic fragility analysis [10].

The piping system, one of the major devices of nuclear power plants, has been considered sufficiently safe against earthquakes, and has thus been classified as "screen out" in probabilistic risk evaluation. When pipes connect structures with seismic isolation devices to general structures, however, it is necessary to consider the seismic anchor motion that occurs at different supports. This is because the seismic risks may be higher compared to the existing piping system as the relative displacement of the pipes with seismic isolation devices will significantly increase. Therefore, it is necessary to evaluate the seismic fragility for such piping system.

To improve the reliability of seismic fragility analysis, it is necessary to define the failure modes and failure criteria considering the performance or functional requirements of the target structure or device [11]. Failure modes can be expressed in various forms, such as the cracking, yielding, and buckling of the structure or device. The purpose of seismic fragility analysis is to predict how, in what situations, and with what degrees of probability the components of the device or structure will be destroyed, and it is extremely important to select the fragile components and to clearly define the failure modes. When the failure modes and failure criteria are defined without clear grounds, inappropriate data capable of inducing errors in fragility evaluation can be used [12].

The current limit state of the design criterion for the pipes installed in nuclear power plants is plastic collapse [13], and the failure of the actual pipes means the leakage caused by the cracks [14]. Therefore, for seismic fragility analysis against critical accidents, such as radiation leakage and reactor core meltdown, research was conducted to propose a quantitative failure criterion for the piping system [15,16]. Research was also conducted to quantitatively identify the failure of the steel pipe elbows using the damage index based on the force-displacement relationship [17]. Based on this, seismic fragility analysis was conducted for the main steam pipe of the APR 1400 nuclear power plant, using the damage index based on the force-displacement relationship [18]. It was confirmed that the damage index based on the force-displacement

relationship can express the failure of the pipe quantitatively and accurately. It is not possible, however, to directly obtain the damage index of the elbow, a fragile component, from the analysis results of the piping system model. As the nonlinear analysis of the piping system must be conducted for seismic fragility analysis, and as nonlinear analysis must be conducted again for the detailed model of the elbow, there is a problem that requires considerable analysis [19].

This study aimed to conduct fragility analysis of the base-isolated piping system using a comparatively simple method. First, the damage index based on the stress-strain relationship (the quantitative failure criterion of the steel pipe elbow) was proposed through experimental and analytical approaches for the 3-inch steel pipe elbow. Modified benchmark model No. 4 [15,19] defined the collapse load point (a criterion for seismic design) and the damage index based on the stress-strain relationship (which represents the actual failure) as failure criteria. It created a seismic fragility curve using the peak ground acceleration (PGA) value as the seismic intensity value. In addition, the seismic fragility curve expressed the collapse load point and damage index simultaneously for the identification of the difference between the design and failure criteria.

2. In-plane cyclic loading test for the 3-inch steel pipe elbow

2.1. 3-Inch steel pipe elbow

In general, the American Society of Mechanical Engineers (ASME)/American National Standards Institute (ANSI) standard piping is applied to nuclear power plant facilities. In the case of large piping such as main steam lines, many tests are difficult to perform and are not economical owing to the limitations of the testing equipment and the high manufacturing cost. In this study, it was confirmed through the previous research and the preliminary analysis that the crown part of the elbow is the fragile part of the piping system [20e22]. Therefore, a piping system composed of an ASME/ANSI 3-inch standard pipe and an elbow was fabricated and used, as shown in Fig. 1, to minimize the fabrication errors as well as the material uncertainties, and to conduct economical research [17,23]. The pipe had a 88.9 mm diameter and a 5.49 mm thickness. To allow plastic behavior to occur in the elbow, straight pipes with a sufficient length of more than 3D (270 mm) were attached to the elbow through welding. In addition, jigs for implementing pin connection were fabricated and attached to both ends of the specimen, also through welding. They were combined using jigs for universal testing machine (UTM) connection.

2.2. In-plane cyclic loading test

Research on the low-cycle fatigue failure of the pipe elbow installed in nuclear power plants was conducted, and it was found that the proper relative displacement applied to the pipe elbow by an earthquake was more than ± 20 mm [24,25]. Therefore, the in-plane cyclic loading test was conducted by applying a 3 MPa internal pressure from ± 20 to ± 90 mm, in which nonlinear behavior occurs, at 10 mm intervals. Fig. 2 shows the steel pipe elbow installed at the UTM for the in-plane cyclic loading test, the image measurement system, the electrical resistance strain gauge, and the air pump for applying the 3 MPa internal pressure. As installing the strain gauge at the installation location of the image measurement system would interfere with the image analysis, the strain gauge was installed at the center of the symmetry plane of the steel pipe elbow for strain measurement [23].

In this study, the failure of the steel pipe elbow was defined as leakage, and the results of the in-plane cyclic loading test indicating

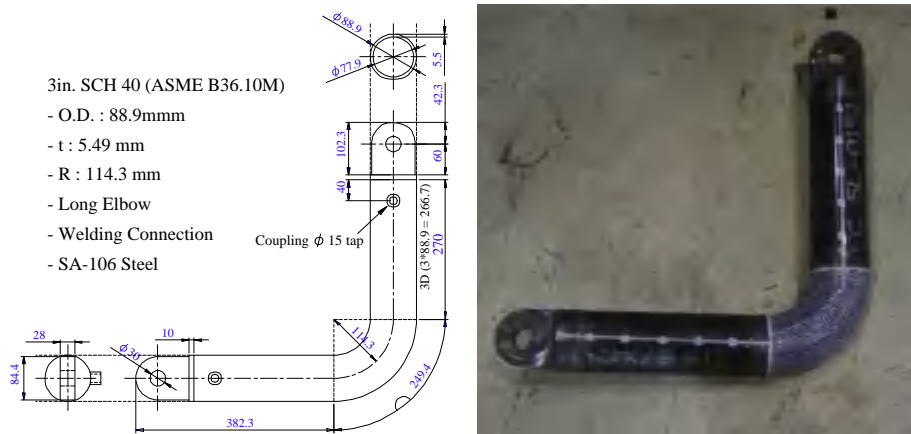


Fig. 1. Steel pipe elbow.

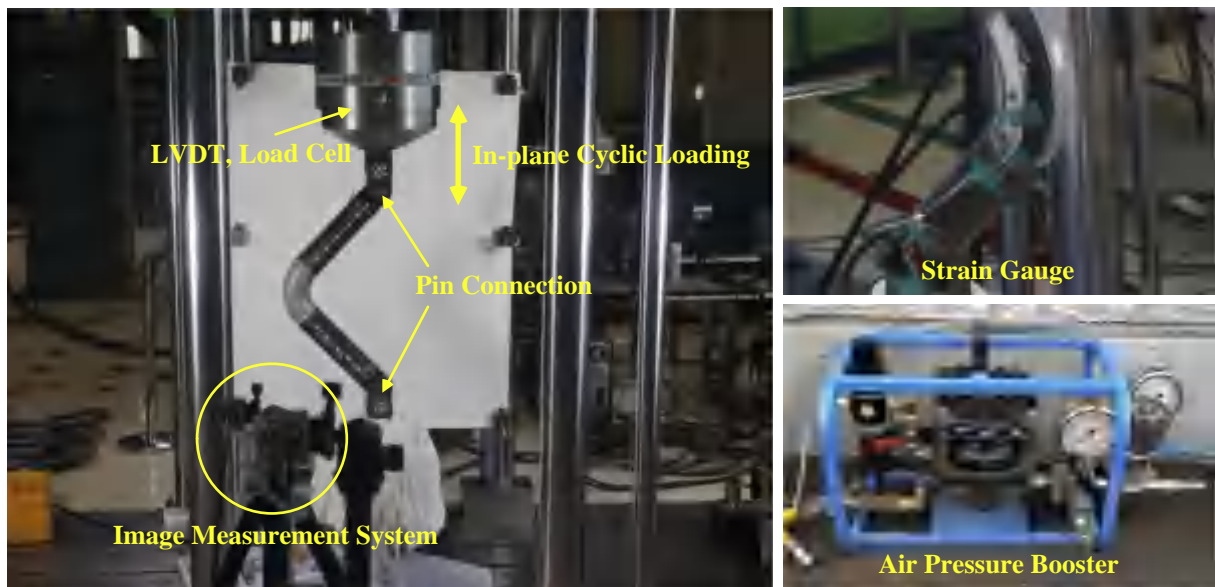


Fig. 2. Sensor installation location.

leakage occurrence are shown in Table 1. As can be seen in the said table, for each load case, the in-plane cyclic loading test was conducted for more than five specimens. Fig. 3 shows the representative steel pipe elbows in which cracks occurred. Such cracks occurred at or near the crown part of the steel pipe elbow.

3. Stress-strain analysis using the finite element model

During the in-plane cyclic loading test, the electrical resistance

Table 1
In-plane cyclic loading test results.

Loading amplitude	Leakage N th cycle	Avg. Leakage cycle
±20 mm	82, 108, 110, 87, 76, 98	94
±30 mm	45, 46, 29, 29, 38	37
±40 mm	17, 18, 18, 14, 15	16
±50 mm	11, 10, 11, 9, 12	11
±60 mm	6, 6, 8, 8, 8	7
±70 mm	4, 5, 5, 4, 6	5
±80 mm	5, 4, 4, 5, 4, 4, 5	4
±90 mm	4, 4, 4, 4, 4	4

strain gauge exceeded its performance limit early after the onset of the nonlinear behavior, and thus could not measure the strain until cracks occurred on the elbow. In the previous study [23], it was confirmed that the strain response measured using the electrical resistance strain gauge and image measurement system has small errors for the data before the performance limit of the strain gauge is reached. In addition, the reliability of the image measurement system was confirmed through a comparison with the results of the electrical resistance strain gauge up to the measurement limit. Thus, the failure strain of the steel pipe elbow in the hoop direction can be measured using the image measurement system. As it was impossible, however, to measure the stress in the hoop direction using the image measurement system, the stress required to define the failure criterion for the piping system was analyzed using finite element model.

For the information required for finite element analysis, the results of the material tensile test conducted in the previous study were used [15,17]. For kinematic hardening, the modulus of elasticity calculated from the material tensile test (204,929 MPa) and the stress-strain curve for nonlinear behavior were used. As shown in Fig. 4, the piping system was modeled using the shell element,



Fig. 3. Steel pipe elbows with cracks.

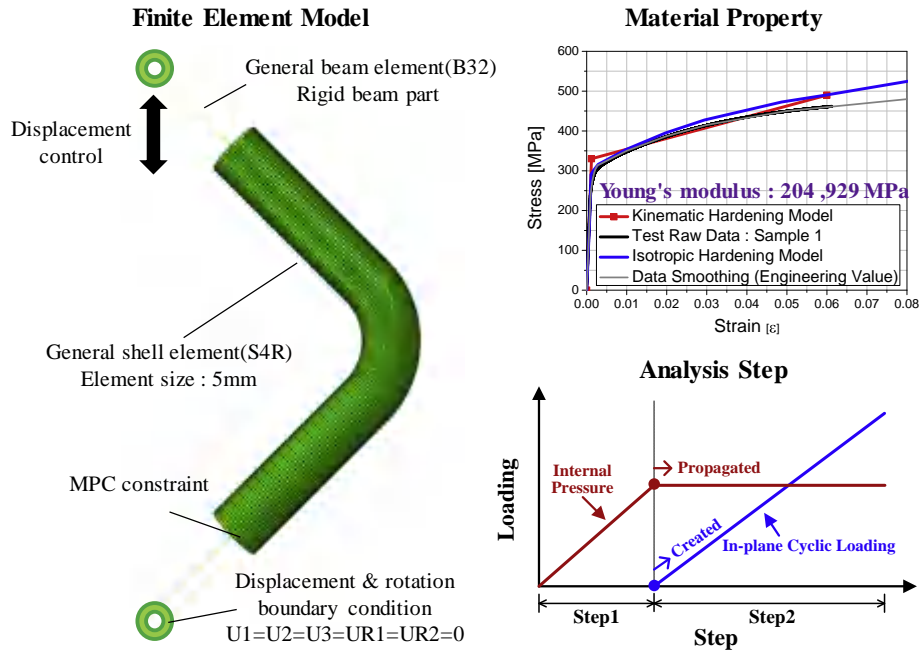


Fig. 4. Finite element analysis.

and the jigs were modeled using the beam element, employing ABAQUS V6.12. The piping system and jigs were connected using MPC beams. The analysis was divided into Step 1 and 2. In Step 1, internal pressure was applied to the piping. Internal pressure was applied to the piping, and the pressure was maintained in step 1. The average leakage cycle, the experiment result shown in Table 1, was inputted as the cycle of the loading amplitude in step 2 for the analysis.

To examine the reliability of the strain response in the hoop direction obtained using finite element analysis, it was compared with the strain response in the hoop direction measured using the image measurement system. Fig. 5 shows the ±60 mm test case of the representative specimen. The force-displacement relationship measured using the load cell and the linear variable differential transformer (LVDT) installed inside the UTM was compared with the analysis results obtained using the finite element model. Fig. 5 (a) shows that the measured force-displacement relationship is in good agreement with the analyzed force-displacement relationship in terms of the initial elastic slope and the nonlinear behavior trend. Fig. 5 (b) shows the strain response in the hoop direction measured using the image measurement system and that obtained through the analysis using the finite element model for the representative specimen shown in Fig. 5 (a). Fig. 5 (b) confirms that the strain in the hoop direction measured using the image

measurement system is in good agreement with the tendency of the strain response determined through analysis at the same position using the finite element model.

4. Damage index of the steel pipe elbow based on the stress-strain relationship

Failure modes can be expressed in various forms, such as the cracking, yielding, and buckling of structures and devices. The purpose of analyzing fragility is to predict how, in what situations, and with what probability levels the components of the target devices and structures will be destroyed. It is important to select fragile elements and to clearly define their failure modes. If the failure modes and failure criteria are defined without clear grounds, inappropriate data capable of inducing errors in fragility evaluation may be used.

The current limit state of the design criterion for the piping system of nuclear power plants is plastic collapse, and actual piping failure occurs due to the leakage caused by penetration cracking. As actual piping failure has never been quantitatively expressed, however, it is difficult to apply it to the seismic fragility analysis of nuclear power plants. Therefore, research was conducted to present a quantitative piping failure criterion for conducting seismic fragility analysis against critical accidents [17].

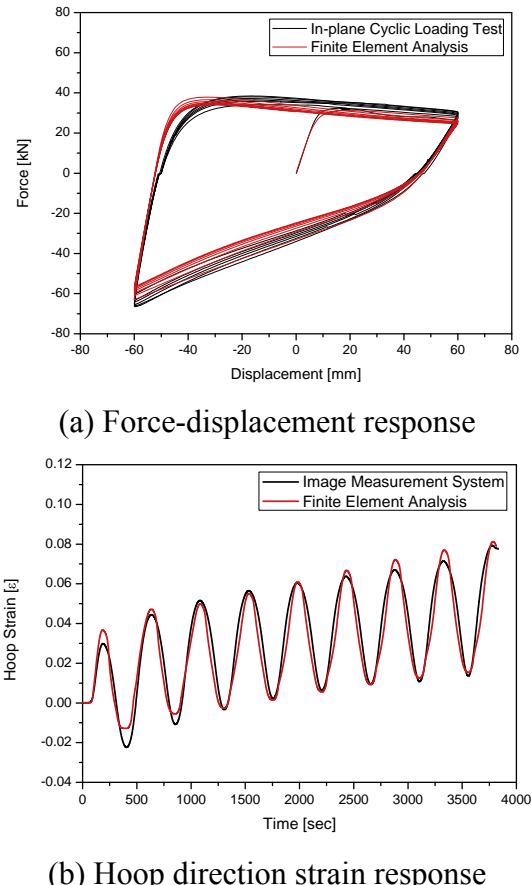


Fig. 5. Comparison of the results in the experiment and finite element analysis: (a) Force-displacement response and (b) Hoop direction strain response.

In the previous study, research on the Banon damage index [26], which is based on the energy dissipation of the force-displacement relationship, was conducted [17]. The application of the Banon damage index as a failure criterion for the seismic fragility evaluation of the piping system, however, involves the following problems. It requires many analysis procedures because the nonlinear seismic response of the piping system must first be analyzed, and then nonlinear analysis of the elbow, a fragile component, must again be conducted. There are problems with the position for evaluating the relative displacement at the elbow, and with the agreement between the displacement response directions in the experiment and analysis. Therefore, in this study, a quantitative failure criterion was defined by developing a modified Banon damage index based on the stress-strain relationship, as shown in Eq. (1), where S_y and ϵ_y are the yield stress and yield strain, respectively; ϵ_i and E_i are the strain and dissipated energy of the i^{th} cycle; and c and d are constants with certain values. The stress and strain in the hoop direction are analyzed using the finite element model, and the damage index is evaluated using the dissipated energy amount. Therefore, the seismic fragility can be evaluated by analyzing the nonlinear seismic response of the piping system.

$$D = \sqrt{\left(\max\left(\frac{\epsilon_i}{\epsilon_u} - 1\right) \right)^2 + \left(\sum_{i=1}^N c \left(2 \frac{E_i}{S_y \epsilon_y} \right)^d \right)^2} \quad (1)$$

For the yield displacement and yield force of the 3-inch steel pipe elbow, the results of the analysis using the finite element model, as shown in Fig. 6 (a), were used. The yield point was

assumed to be the intersection between the extension of the slope of initial stiffness and that of the slope of plastic stiffness [27]. In this instance, the yield load and yield displacement were found to be 28 kN and 9 mm, respectively. As shown in Fig. 6 (b), the yield point of the stress-strain relationship was inferred from the analysis results. The yield strain was 0.00185, and the yield stress was 440 MPa. For c and d , which are the constants of the Banon damage index, 3.3 and 0.21, respectively, were applied through optimization using the experiment results.

According to the results of the previous study, the elbow crack occurs inside the crown and grows in the axial direction [17,23]. Strain and low-cycle ratcheting fatigue damage in the hoop direction were observed. Therefore, in this study, the failure criterion for the elbow was defined using the hoop direction stress-strain response. Finite element analysis was conducted using the average leakage cycle from the results of the in-plane cyclic loading test. As shown in Fig. 7, the degree of damage was expressed by applying the hoop direction stress-strain response at the position of the elbow's crown to the modified Banon damage index.

Fig. 8 confirms that the damage indices based on the stress-strain relationship converged well to a certain level for each loading amplitude, and indicates that the modified Banon damage index can be used as a failure criterion for seismic fragility analysis.

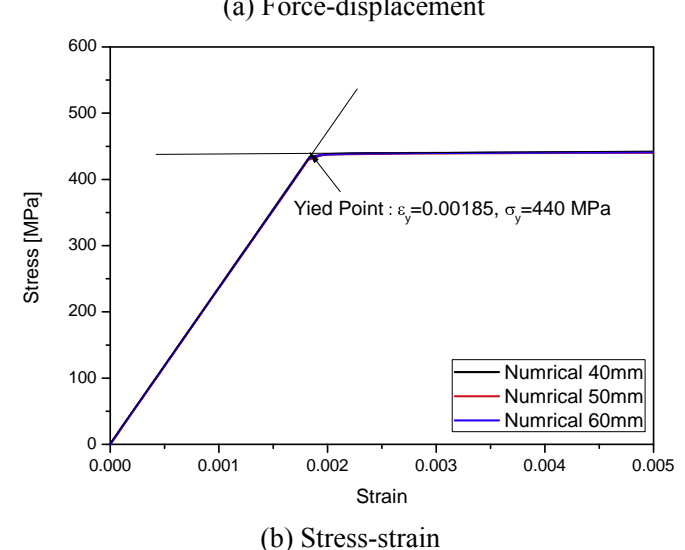
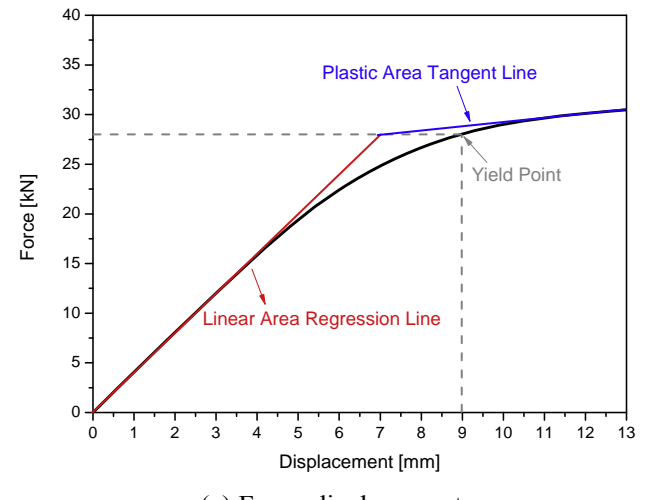
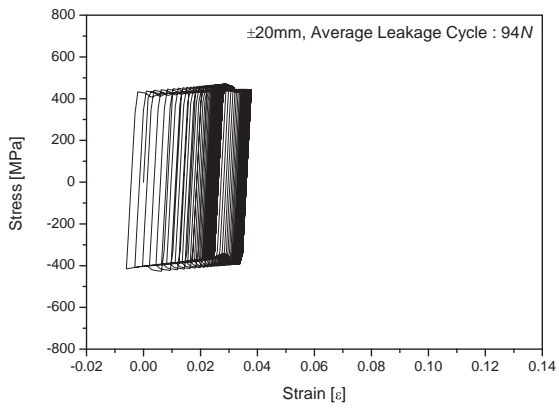
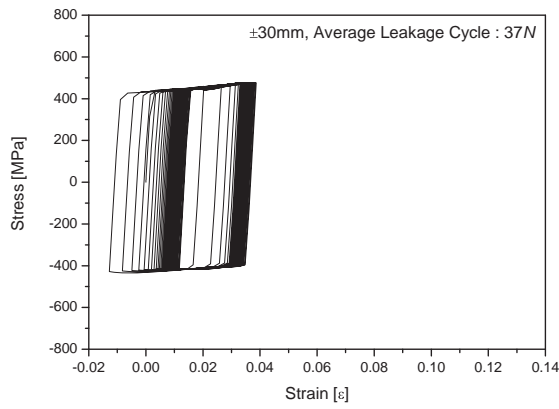


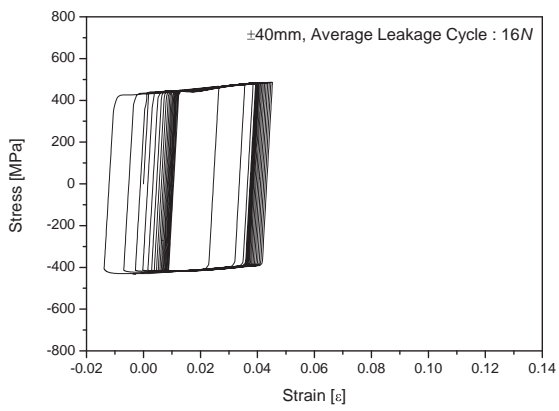
Fig. 6. Yield point of the 3-inch steel pipe elbow analyzed in the finite element model: (a) Force-displacement and (b) Stress-strain.



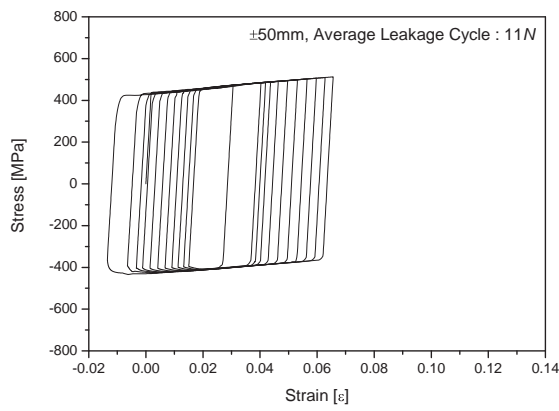
(a) ± 20 mm



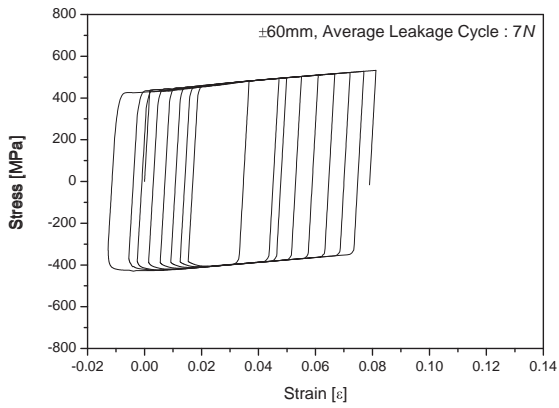
(b) ± 30 mm



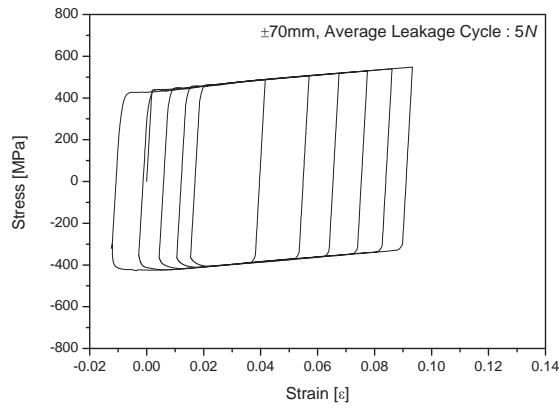
(c) ± 40 mm



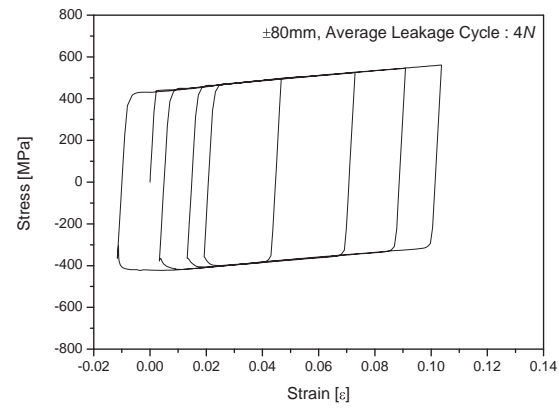
(d) ± 50 mm



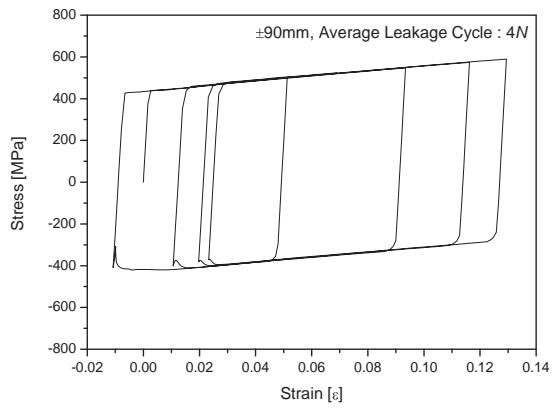
(e) ± 60 mm



(f) ± 70 mm



(g) ± 80 mm



(h) ± 90 mm

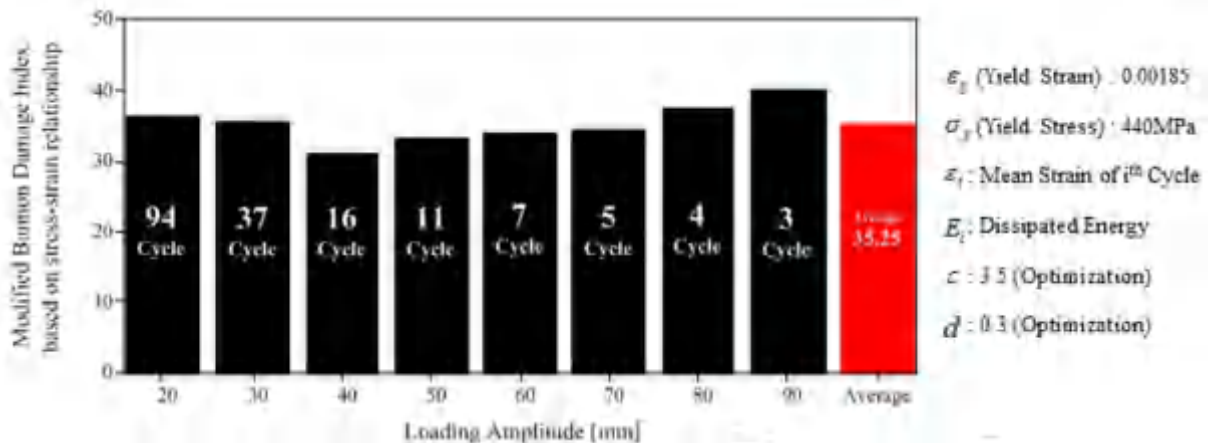


Fig. 8. Modified Banon damage index of the steel pipe elbow.

Fig. 9 compares the Banon damage index based on the force-displacement relationship [17] with the modified Banon damage index based on the stress-strain relationship. The two bars in Fig. 9 represent the Banon damage index and modified Banon damage index, respectively, confirming their similar tendencies. Therefore, it seems possible to quantitatively express the failure of the steel pipe elbow (i.e., leakage caused by cracks).

5. Seismic fragility evaluation for the base-isolated nuclear power plant piping system

In this study, seismic fragility analysis was conducted for the piping system considering a leakage accident, a critical accident, as a failure criterion. The failure of the piping system was quantitatively defined using the damage index based on load displacement, and the seismic fragility analysis was conducted for the main steam piping system of the APR1400 nuclear power plant [18]. For conducting seismic fragility analysis using the damage index based on force-displacement, however, many interpretations are required, as mentioned in section 4. Therefore, the damage index based on stress-strain was defined as a failure criterion for conducting economic seismic fragility analysis.

The collapse load point and the modified Banon damage index based on the hoop direction stress-strain relationship, which was obtained using finite element analysis, were defined as the failure criteria for modified benchmark model No. 4 [15,19]. A seismic fragility curve was created using the PGA value as the seismic intensity value. The seismic fragility curve expressed the collapse load point and the damage index simultaneously for the identification of the difference between the design and failure criteria.

5.1. Seismic response analysis

In this study, nonlinear seismic response analysis was conducted using the modified NRC-BNL benchmark model no. 4, which was proposed to exhibit characteristics similar to those of the structures and piping systems of nuclear power plants, as shown in Fig. 10. The resulting floor response was applied to each point of the modeled piping system as a shell element for conducting nonlinear seismic response analysis. Table 2 shows the assumptions for the material property, dynamic characteristics, and seismic isolation

devices of the finite element model of the modified NRC-BNL benchmark model no. 4.

If seismic isolation devices are introduced to a nuclear power plant, a relatively larger displacement may occur as such devices handle the load caused by an earthquake, and as such, it is likely that the seismic risks of the connected piping system will increase sharply. Therefore, it was deemed necessary in this study to focus on the horizontal displacement response of the structure in conducting seismic fragility analysis for piping systems connected to some base-isolated nuclear power plants. In addition, as Nuclear Regulatory Commission Regulation (NUREG) recommends that seismic fragility analysis be conducted using proper variables (e.g., horizontal displacement) for piping systems that are sensitive to the displacement of base-isolated nuclear power plants, seismic fragility analysis was conducted only in the horizontal Z-axis direction.

As specific target areas were not determined in this study, five artificial time histories and spectrum-matched input ground motions were produced and used to meet the ASCE 43-05 regulations [28,29]. These had the unsteady characteristics of actual seismic waves and considered the various conditions of such waves. The five artificial time histories [30] that were produced and used in this study included the various conditions of inter-plate earthquakes, intra-plate earthquakes, earthquakes with pulse-type close-range seismic characteristics, and earthquakes measured in the hanging and foot wall areas, and targeted the selected seed earthquake. The input ground motions that were produced and used in this study, on the other hand, were created using RspMatch, the software developed by Hancock et al. [31], to fit the horizontal-direction 5% damping spectrum of Regulatory Guide (RG) 1.60, whose PGA is 0.5 g. Fig. 11 shows the target response spectrum for the horizontal direction (Z direction) and the response spectra for the deformed time histories. Table 3 shows the information on the seed earthquake. Fig. 11 shows that the zero period acceleration (ZPA) is somewhat higher than 0.5 g. This difference, however, was shown not to have significantly affected the analysis that was conducted to examine the failure mode of the piping system in which damage occurs due to the low-frequency dynamic loads, because it occurred in the frequency range higher than approximately 30 Hz. The acceleration magnification of the input seismic wave was amplified to analyze the nonlinear seismic response, and the measurement points were P1, P2, P3, and TOP, as shown in Fig. 12.

Fig. 7. Hoop direction stress-strain response analyzed at the crown of the steel pipe elbow using the finite element model: (a) ± 20 mm; (b) ± 30 mm; (c) ± 40 mm; (d) ± 50 mm; (e) ± 60 mm; (f) ± 70 mm; (g) ± 80 mm; and (h) ± 90 mm.

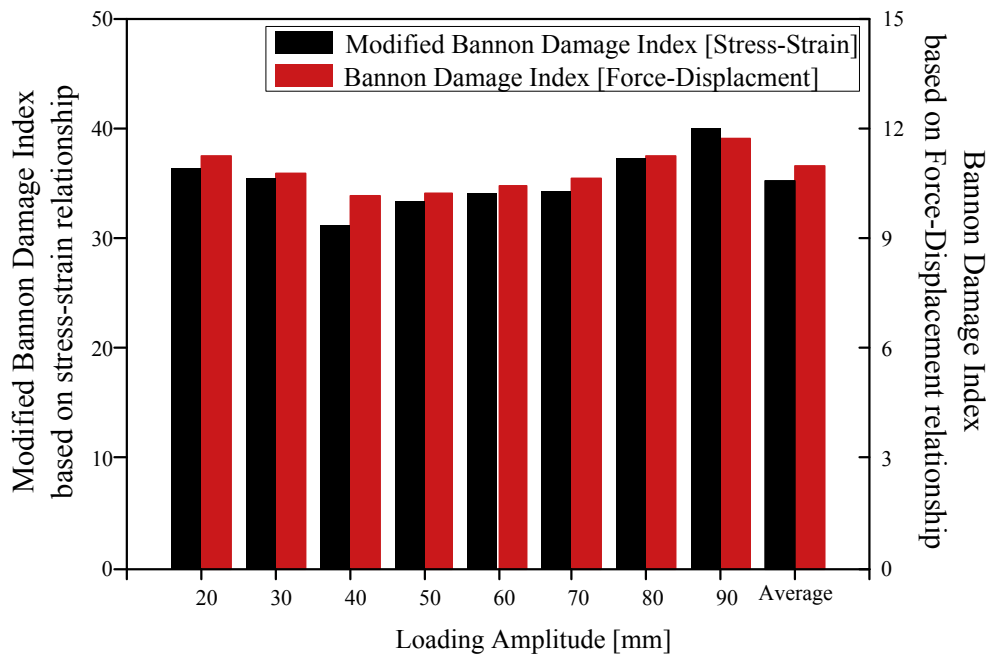


Fig. 9. Comparison of the modified Bannon damage index and the Bannon damage index of the steel pipe elbow.

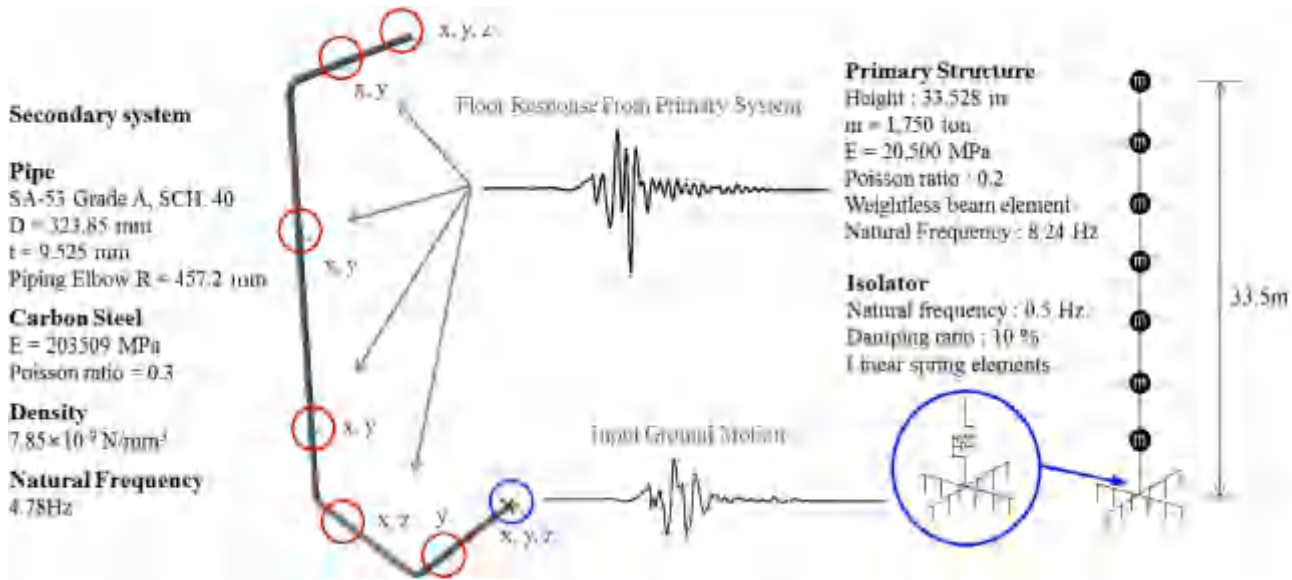


Fig. 10. Seismic response analysis for the base-isolated nuclear power plant piping system.

The finite element model of the piping system was modeled using S8R5, which is the shell element of ABAQUS 6.12 capable of expressing the elliptical deformation and distortion of piping. The elements numbered 26,425, and the nodes, 26,450. For piping, the outer diameter was 323.9 mm, the thickness was 9.5 mm, and the turning radius of the curved pipe was 457.2 m. These correspond to the ASME B36.10M, SA53, Grade A, and SCH 40 carbon steel. The material properties determined through the element experiment and the finite element model were used. The damping ratio was assumed to be 4% by referring to the piping system damping ratio based on the safe shutdown earthquake (SSE) of RG 1.61. The created finite element model of the piping system is shown in Fig. 13, and the boundary conditions are listed in Table 4. Table 5 shows the natural frequencies for each mode, which are the

eigenvalue analysis results for the finite element model of the piping system.

For nonlinear seismic response analysis, 6.31 MPa internal pressure was applied in Step 1, using ABAQUS 6.12 [15,19]. While the stress caused by the internal pressure in Step 1 was propagated, seismic response analysis was conducted in Step 2 using the implicit method, a direct integration method. For the seismic wave in Step 2, the displacement in the DZ direction was excited. The time increment was fixed at 1/64 s for the analysis using the Newton-Raphson method.

5.2. Seismic fragility analysis

Seismic fragility analysis was conducted using the collapse load

Table 2
Modified NRC-BNL benchmark model No. 4

	Fundamental natural frequency	Elements	Remarks
Primary structure	8.92 Hz	Beam	Lumped mass: 17150 kN Poisson's ratio: 0.2 Elastic modulus: 21 GPa
Piping system	4.77 Hz	Shell	Poisson's ratio: 0.3 Elastic modulus: 204 GPa External diameter: 323.85 mm Thickness: 10.1 mm Radius: 457.2 mm
Isolation device	0.50 Hz	Spring Dashpot	Damping ratio: 4% (Rayleigh damping) LDR (Low-damped Rubber bearing) + Linear viscous damper

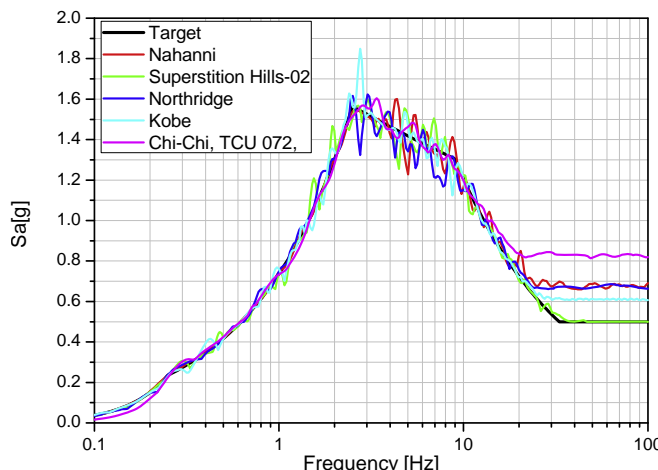


Fig. 11. Target response spectrum and response spectra for five deformed time histories (Z-axis).

point and the modified Banon damage index as failure criteria, and the following conditions were considered. From the results of the application of the monotonic load to the piping, 0.004 strain, which was the stricter value of the collapse load points of the closing and opening modes, was defined as collapse [32]. In the case of the SCH40 piping of the same material, it was assumed that the damage index value for failure was identical [33], and thus, the modified Banon damage index based on the stress-strain relationship was used as a failure criterion. The uncertainty coefficient for the capacity was induced using the results of the finite element analysis of the piping system. For the uncertainty coefficient, the nonlinear analysis results of the 3-inch piping system by loading amplitude were evaluated using the modified Banon damage index.

For the seismic fragility curve, the form of the log-normal distribution function is appropriate. The two important variables of seismic fragility with the form of a two-parameter log-normal distribution are the median value and the log-normal standard deviation. In general, when an arbitrary seismic load a is applied,

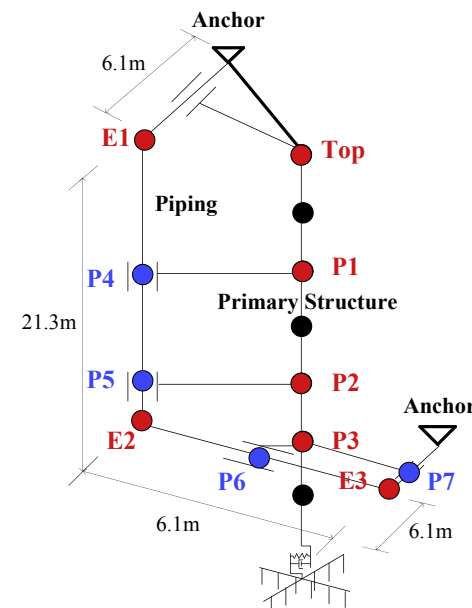


Fig. 12. Measurement points for examining the seismic response analysis results.

the damage probability of the structure can be defined as Eq. (2). In Eq. (2), p_R is the probability density function of the response, and p_C is the probability density function of the capacity.

$$P_f(a) = \int_0^{\infty} p_R(a; x_R) \left[\int_0^{x_R} p_C(x) dx \right] dx_R \quad (2)$$

Eq. (2) can be expressed as Eq. (3) considering the uncertainties of the capacity and the response [12]. C_m is the median value of the capacity (median performance value), R_m is the median value of the structure response, $F(\cdot)$ is the cumulative probability distribution of the standard normal distribution function, and b_C is the log-normal standard deviation of the compound random variable.

$$P_f(a) = 1 - F\left[\frac{\ln C_m - \ln R_m(a)}{b_C}\right] \quad (3)$$

b_C in Eq. (3) can be expressed as the square root of the sum of squares of log-normal standard deviation b_R of the random variables, which considers the randomness, and of log-normal standard deviation b_U , which means uncertainty, as shown in Eq. (4).

$$b_C = \sqrt{b_R^2 + b_U^2} \quad (4)$$

Table 3
Seed earthquake for creating spectrum-matched input ground motions.

No.	Earthquake	Station	Inter/Intra	Mw	Distance [km]
1	Nahanni	S3	Intra	6.76	5.32
2	Superstition Hills-02	ICC	Inter	6.54	18.2
3	Northridge	PKC	Inter	6.69	7.26
4	Kobe	KJMA	Inter	6.90	0.96
5	Chi-Chi, Taiwan	TCU072	Inter	7.62	7.03

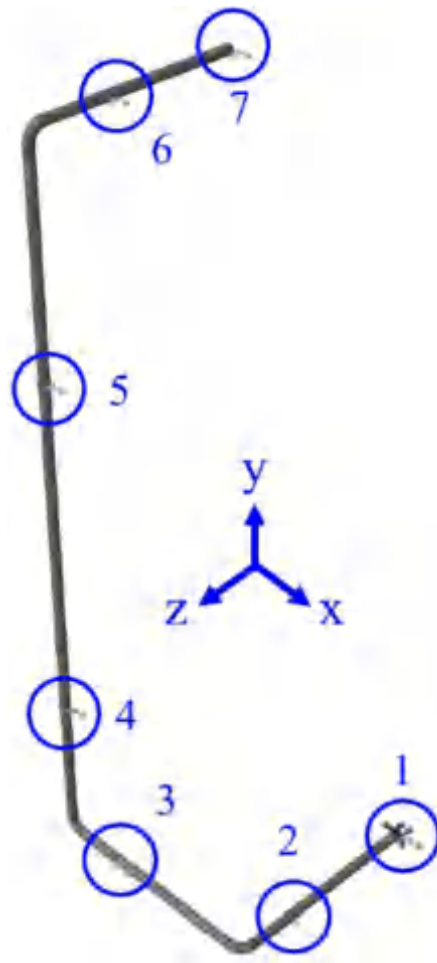


Fig. 13. Finite element model of the piping system.

Table 4
Boundary conditions of the finite element model.

Support ID	Restraint Direction
1, 7	DX, DY, DZ, Rx, Ry, Rz
4, 5, 6	DX, DY
3	DX, DZ
2	DY

Although the log-normal standard deviation of the compound random variables is an important coefficient that plays a decisive role in the fragility response, the grounds for it are still insufficient. In this study, the log-normal standard deviations of uncertainty and randomness (b_U and b_R) were induced from the results of the in-plane cyclic loading test and the nonlinear seismic response analysis for the piping system. The log-normal standard deviation of uncertainty, b_U , represents the uncertainty of the capacity. The nonlinear analysis results of the 3-inch piping system by loading amplitude were evaluated using the modified Banon damage index of the steel pipe elbow, and then the log-normal standard deviation of the damage index values (0.033) was used. The log-normal standard deviation of randomness, b_R , represents the randomness of the response, and it was induced using the results of the nonlinear seismic response analysis. In general, the given coefficient of variation of the input seismic wave is applied to reflect the

Table 5
Natural frequencies of the piping system for each mode.

Mode	Frequency [Hz]	Direction
1	4.772	Z
2	8.726	Z
3	17.050	X
4	17.820	X
5	22.797	Z

characteristics of various earthquakes with an undefined spectrum. As a seismic wave suitable for the design response spectrum was excited in this study, however, the variability of the input seismic wave was smaller, and it was deemed appropriate to use a seismic wave suitable for the design response spectrum to examine the performance of the structure. In addition, as it was assumed that the distribution of the response followed the log-normal distribution, the log-normal standard deviation was applied to the coefficient of variation.

The seismic fragility curve was created using the collapse load point and the modified Banon damage index as failure criteria, and the fragility curve was shown in the same graph for comparative analysis. Fig. 14(a) shows the seismic fragility curve created by applying the collapse load point as a failure criterion, and Fig. 14(b) shows the seismic fragility curve created by applying the collapse load point and the modified Banon damage index as failure criteria. When the collapse load point capable of covering the seismic design criteria was used as a failure criterion, the median value of the failure probability was considerably low compared to the case in which the modified Banon damage index representing the actual failure was used as a failure criterion. Therefore, for the seismic fragility evaluation of the piping system, it is deemed appropriate to apply the damage index capable of representing the actual failure as a failure criterion.

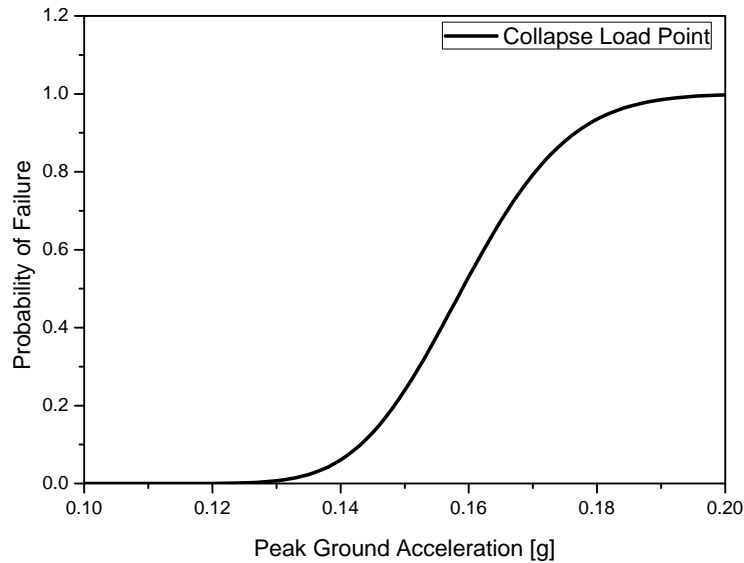
6. Conclusions

In this study, seismic fragility analysis was conducted against a leakage accident, which may cause a critical accident in the piping system of a base-isolated nuclear power plant, using the damage index based on stress-strain. In addition, the actual pipe leakage accident was compared with the results of the seismic fragility analysis, where plastic collapse was considered a failure criterion.

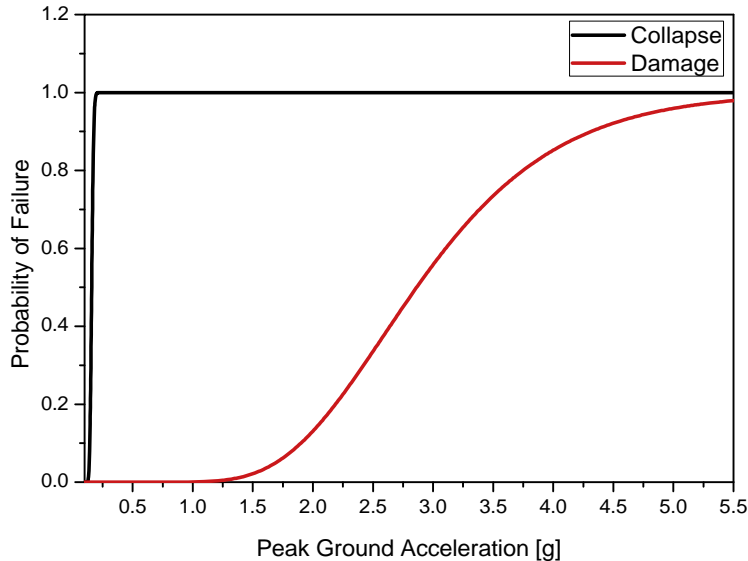
To quantitatively define the limit state of the steel pipe elbow, which is the fragile element of the piping system, using the experimental and analytical methods, the in-plane cyclic loading test was conducted for the 3-inch steel pipe elbow using various loading amplitudes. It was found that the loads, loading amplitudes, and hoop direction strains measured in the in-plane cyclic loading test were in good agreement with the results of the analysis conducted using the finite element model.

This study proposed a damage index that can quantitatively express the actual failure of the steel pipe elbow, and defined the failure caused by the leakage of the piping system. It was confirmed that the actual failure can be quantitatively expressed using the modified Banon damage index based on the stress-strain relationship. Seismic fragility analysis for the piping system was conducted using the failure criteria proposed through the experimental and analytical methods, and the collapse load point and the modified Banon damage index were used as failure criteria.

When the collapse load point, a seismic design criterion, was applied as a failure criterion, the median value of the failure probability was found to be considerably low compared to the case



(a) Seismic fragility curve using the collapse load point as a failure criterion



(b) Seismic fragility curve comparison depending on the failure criterion

Fig. 14. Seismic fragility evaluation for the base-isolated benchmark model No. 4 piping system: (a) Seismic fragility curve using the collapse load point as a failure criterion and (b) Seismic fragility curve comparison depending on the failure criterion.

in which the damage index representing the actual failure was applied as a failure criterion. In addition, the collapse load point, a design criterion, was found not to be appropriate for application as a failure criterion for the seismic fragility analysis of the piping system, because it exhibited a large difference in terms of the time at which leakage occurred in the component test. Therefore, if the seismic fragility evaluation of the piping system is performed by applying the stress-strain-based damage index, which can represent the damage of the actual piping, as a failure criterion, it will be possible to derive economical and reliable results.

Conflicts of interest

All authors have no conflicts of interest to declare.

Acknowledgements

This work was supported by the National Research Foundation of Korea (NRF) grant funded by the Korea government (NRF-2017M2A8A4039749). Moreover, the authors would like to thank the KOCED Seismic Research and Test Center for their assistance with the test equipment.

References

- [1] A.M. Kammerer, A.S. Whittaker, M.C. Constantinou, Technical Considerations for the Seismic Isolation of Nuclear Facilities," NUREG/CR-xxxx, United States Nuclear Regulatory Commission, Washington, D.C. 2017.
- [2] R. Burby, R. Deyle, D. Godschalk, R. Olshansky, Creating Hazard Resilient Communities through land-use Planning, *natural Hazards Review*, vol. 1, ASCE, 2000, pp. 99e106.

- [3] M. Lindell, C. Prater, Assessing Community impacts of natural disasters, *Nat. Hazards Rev.* 4 (2003) 176e185.
- [4] J.Y. Park, K.S. Jan, H.P. Lee, Y.H. Lee, Kim, Experimental study on the temperature dependency of full scale low Hardness lead Rubber bearing, *J. Comput. Struct. Eng. Ins. Korea* 25 (2012) 533e540.
- [5] J.M. Kelly, A seismic base isolation: Review and bibliography, *Soil Dynam. Earthq. Eng.* 5 (1986) 202e216.
- [6] N. Kani, Current state of seismic-isolation design, *J. Disaster Res.* 4 (2008) 175e181.
- [7] M. Forni, A. Poggianti, F. Bianchi, G. Forasassi, R. Lo Frano, G. Pugliese, F. Perotti, L. Corradi dell'Acqua, M. Domaneschi, M.D. Carelli, M.A. Ahmed, A. Maioli, Seismic isolation of the IRIS nuclear plant, in: ASME 2009 Pressure Vessels and Piping Conference, American Society of Mechanical Engineers, Prague, Czech Republic, 2009. PVP2009-78042.
- [8] F. Perotti, M. Domaneschi, S.D. Grandis, The numerical computation of seismic fragility of base-isolated nuclear power plants buildings, *Nucl. Eng. Des.* 262 (2013) 189e200.
- [9] H.P. Lee, M.S. Cho, A study on the Reduction effect for seismic isolation system of nuclear power plant, in: Proceedings of the 15 World Conference on Earthquake Engineering, Lisbon, Portugal, 2012, p. 30608.
- [10] S.H. Eem, H.J. Jung, Seismic fragility assessment of isolated structures by using stochastic response database, *Earthquakes and Structures* 14 (2018) 389e398.
- [11] I. Nakamura, N. Kasahara, Excitation tests on elbow pipe specimens to investigate failure behavior under excessive seismic loads, in: ASME 2015 Pressure Vessels and Piping Conference, Boston, Massachusetts, USA, 2015. PVP2015-45711.
- [12] M.K. Kim, O. Yasuki, Y.S. Choun, I.K. Choi, Analysis of seismic fragility improvement effect of an isolated rotational equipment, *J. Earthquake Eng. Soc. Korea* 11 (2007) 69e78.
- [13] ASME Boiler & Pressure Vessel Code, 2007.
- [14] N. Kasahara, I. Nakamura, H. Machida, H. Nakamura, Research plan on failure modes by extreme loadings under design extension conditions, in: ASME 2014 Pressure Vessels and Piping Conference, Anaheim, California, USA, 2014. PVP2014-28349.
- [15] B.G. Jeon, Seismic Fragility Evaluation of Base Isolated Nuclear Power Plant Piping System (Ph.D. thesis), Pusan National University, 2014.
- [16] B.G. Jeon, H.S. Choi, D.G. Hahn, N.S. Kim, Seismic fragility analysis of base isolated NPP piping systems, *J. Earthquake Eng. Soc. Korea* 19 (2015) 29e36.
- [17] B.G. Jeon, S.W. Kim, H.S. Choi, D.U. Park, N.S. Kim, A failure estimation method of steel pipe elbows under in-plane cyclic loading, *Nucl. Eng. Technol.* 49 (2017) 245e253.
- [18] E.S. Firoozabad, B.G. Jeon, D.G. Hahn, N.S. Kim, Seismic fragility of APR1400 main steam piping system, in: 13th International Conference on Probabilistic Safety Assessment and Management (PSAM 13), Seoul, Korea, 2016. A-576.
- [19] E.S. Firoozabad, B.G. Jeon, H.S. Choi, N.S. Kim, Seismic fragility analysis of seismically isolated nuclear power plants piping system, *Nucl. Eng. Des.* 284 (2015) 264e279.
- [20] I. Nakamura, A. Otani, M. Shiratori, Comparison of failure modes of piping systems with wall thinning subjected to in-plane, out-of-plane, and mixed mode bending under seismic load: an experimental approach, *ASME J. Pressure Vessel Technol.* 132 (2010) 031001.
- [21] G.E. Varelis, S.A. Karamanos, A.M. Gresnigt, Pipe elbows under strong cyclic loading, *ASME J. Pressure Vessel Technol.* 135 (2013) 011207.
- [22] K. Yoshino, R. Endou, T. Sakaida, H. Yokota, T. Fujiwaka, Y. Asada, K. Suzuki, Study on seismic design of nuclear power plant piping in Japan-Part 3: component test results, in: ASME 2015 Pressure Vessels and Piping Conference, ASME, 2015, pp. 131e137.
- [23] S.W. Kim, B.G. Jeon, H.S. Choi, D.G. Hahn, M.K. Kim, Strain and deformation angle for a steel pipe elbow using image measurement system under in-plane cyclic loading, *Nucl. Eng. Technol.* 50 (2018) 190e202.
- [24] K. Takahashi, S. Watanabe, K. Ando, A. Hidaka, M. Hisatsune, K. Miyazaki, Low cycle fatigue behaviors of elbow pipe with local wall thinning, *Nucl. Eng. Des.* 239 (2009) 2719e2727.
- [25] Y. Urabe, K. Takahashi, K. Sato, K. Ando, Low cycle fatigue behavior and seismic assessment for pipe bend having local wall thinning-influence of internal pressure, *J. Pressure Vessel Technol.* 135 (2013) 2e6.
- [26] H. Banon, H.M. Irvine, J.M. Biggs, Seismic damage in reinforced concrete frames, *J. Struct. Div.* 107 (1981) 1713e1729.
- [27] J. Gersák, Study of the yield point of the thread, *Int. J. Cloth. Sci. Technol.* 10 (1989) 244e251.
- [28] J.H. Kim, M.K. Kim, I.K. Choi, Response of base isolation system subjected to spectrum matched input ground motions, *J. Earthquake Eng. Soc. Korea* 17 (2014) 89e95.
- [29] ASCE, Seismic Design Criteria for Structures, Systems, and Components in Nuclear Facilities, ASCE 43-05, ASCE, Reston, Virginia, USA, 2005.
- [30] ASCE, Seismic Analysis of Safety-related Nuclear Structures and Commentary, ASCE 4-98, ASCE, Reston, Virginia, USA, 2000.
- [31] J. Hancock, J. Watson-Lamprey, N.A. Abrahamson, J.J. Bommer, A. Markatis, E. McCoy, R. Mendis, An improved method of matching response spectra of recorded earthquake ground motion using wavelets, *J. Earthq. Eng.* 10 (2006) 67e89.
- [32] B.G. Jeon, H.S. Choi, D.G. Hahn, N.S. Kim, Seismic fragility evaluation of base isolated nuclear power plant piping system, in: Proceedings of the ICTWS 2014 7th International Conference on Thin-walled Structures ICTWS2014, Busan, Korea, 2014. ICTWS2014-0901.
- [33] E.S. Firoozabad, B.G. Jeon, H.S. Choi, N.S. Kim, Failure criterion for steel pipe elbows under cyclic loading, *Eng. Fail. Anal.* 66 (2016) 515e525.